Regular Article

PHYSICAL CHEMISTRY RESEARCH
Published by the
Iranian Chemical Society
www.physchemres.org
info@physchemres.org

***Phys. Chem. Res.**, Vol. 5, No. 3, 439-446, September 2017*
DOI: 10.22036/pcr.2017.72834.1347

Thermodynamics and Kinetics of Spiro-Heterocycle Formation Mechanism: Computational Study

A.A. Siaka*, A. Uzairu, S. Idris and H. Abba

Department of Chemistry, Ahmadu Bello University, P.M.B 51, Zaria 810001, Kaduna, Nigeria

(Received 13 January 2017, Accepted 21 February 2017)

Reaction mechanism among indoline-2,3-dione, pyrrolidine-2-carboxylic acid and (Z)-2-(1-(2-hydroxynaphthalen-1-yl)ethylidene) hydroxy-carboxamide to form 1'-((((aminooxy)carbonyl)amino)methyl)-2'-(1-hydroxynaphthalen-2-yl)-2'-methyl-1',2',5',6',7',7a'-hexahydrospiro[indoline-3,3'-pyrrolo[1,2-a]imidazole-2-one was investigated using density functional theory (DFT) at B3LYP level of theory. The three-step reaction occurred *via* five stationary points, including two van der Waals complexes (1 and 2), two intermediates and one transition state. The entropy change across the various steps indicated an appreciable interaction or overlap within the reacting molecules. This was also evident in variations in the geometries of the optimized species as the reaction progressed from the intermediates through the transition state to the final product. The steps leading to the formation of van der Waals complexes (1 and 2) were thermodynamically feasible in contrast to the bimolecular transition step. From the equilibrium constant value, the transition step was found to be the rate-determining step. The study is able to provide information on the energetics of the individual step of the reaction and the overall process in addition to change in geometries as the initial reacting molecules transformed through the saddle points to the final product.

Keywords: Mechanism, Bimolecular, van der Waals complexes, Geometries and entropy

INTRODUCTION

Naturally occurring and synthesized compounds are found to have spiro type structures and many have become drug candidates. The last two decades have witnessed the increase in the number of research works on the synthesis and biological importance of spiro derivatives with the objective of uncovering the core elements necessary for the biological significance. One of the natural substances with highly pronounced bioactivities is spiro-oxindole ring system [1], including abamectin [2], chlorogenin [3] and illudins [4]. Compounds with 1,2,4-triazole fused ring are characterized with high biological properties as antimicrobial, anticonvulsant, antidepressant, antihypertensive, antitumarial and analgesic agents [5,6]. Furthermore, mild hypertension can be treated effectively without the risk of hypokalemia or increased secretion of aldosterone inducement by using spironolactone [7].

*Corresponding author. E-mail: fatsaadaby@gmail.com

Spiro-cyclic compounds have attracted the attention of organic chemists due to their unique structural and reactivity pattern. Literature is rich on reactions involving biologically significant organic molecules (*e.g.* spiroheterocycles), and quite a percentage of these reactions do not have explicit reaction mechanisms. Preparation of spiro-heterocycles using indolin-2,3-dione and pyrrollin-2-carboxylic acid without detailed mechanism was reported by Scholastica *et al.,* 2012 [8].

To the best of our knowledge, thermodynamics and kinetics of formation of this important biological molecule has not been investigated yet. Therefore, this study attempts to provide such information using theoretical and computational methods.

EXPERIMENTAL

Computation Methods

Cascading computational procedure method was applied for optimization and calculation of all the geometries in this

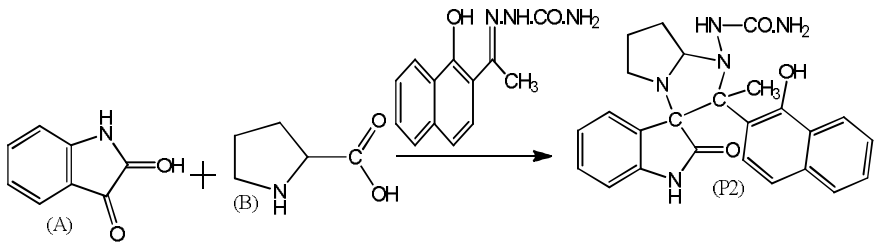

Fig. 1. General scheme for indoline-2,3-dione, pyrrolidine-2-carboxylic acid and (Z)-2-(1-(2-hydroxy-naphthalen-1-yl)ethylidene)hydroxycarboxamide reaction system.

work. The "cascade method" uses the molecular mechanics to remove strain energies; this is followed by application of semi-empirical method and finally the more exact DFT method [9]. This method is significant because it has the ability to make computation less demanding by relegating initial geometry calculation to less intensive computational methods. The formation enthalpies of all the stationary points were computed using thermochemical recipe at T_1 theory level. Thermochemical recipe at T1 theory level is a composite scheme based on single-point energies, *i.e.*, RRIMP2(FC/6-311++G(2df,2p)[6-311G*] [10]. Analytic frequency computation was employed to confirm the nature of all the stationary points (intermediates and transition states) and the transition states were characterized by imaginary frequencies. Intrinsic reaction coordinate calculations were carried out at B3LYP/6-311++G** [11] to confirm that the transition states connect to the right minima.

Thermodynamic and kinetic parameters of the reaction mechanism were calculated using the expressions below as reported in [12]. The enthalpies of reactions were evaluated using the formulation;

$$\Delta_r H^o(298.15K) = \sum_{prod} n_{prod}\Delta_f H^o_{prod}(298.15K) - \sum_{react} n_{react}\Delta_f H^o_{react}(298.15K) \quad \text{(i)}$$

where n_{prod} and n_{react} are the stoichiometric coefficients of the products and reactants respectively, while $\Delta_f H^\circ_{react}(298.15K)$, $\Delta_f H^\circ_{prod}(298.15K)$ and $\Delta_r H^\circ(298.15K)$, are the standard heat of formation of reactants, standard heat of formation of products and standard heat of reaction, respectively, at the specified temperature.

The reaction entropy was calculated from the expression as thus;

$$\Delta_r S^o(298.15K) = \sum_{prod} n_{prod} S^o_{prod}(298.15K) - \sum_{react} n_{react} S^o_{react}(298.15K) \quad \text{(ii)}$$

where n_{prod} and n_{react} are the stoichiometric coefficients of the products and reactants respectively, while $S^\circ_{react}, S^\circ_{prod}$ *and* $\Delta_r S^\circ$ are the standard entropy of reactants, standard entropy of products and standard entropy of reaction, respectively, at the specified temperature.

The Gibbs energy can be calculated using the expressions below:

$$\Delta_r G^o = \Delta_r H^o - T\Delta_r S^o \quad \text{(iii)}$$

$$\Delta G^{\#}_{(298.15K)} = \Delta H^{\#} - T\Delta S^{\#} \quad \text{(iv)}$$

$$k_{(298.15K)} = \frac{k_B T}{hC^o} e^{\Delta S^{\#}/R} e^{-\Delta H^{\#}/RT} \quad \text{(v)}$$

$$K_{(298.15K)} = e^{-\Delta G^{\#}/RT} \quad \text{(vi)}$$

$A = \frac{e^2 k_B T}{hc^\circ} e^{\frac{\Delta S^{\neq}}{R}}$, for bimolecular (vii)

$A = \frac{e^2 k_B T}{hc^\circ} e^{\frac{\Delta S^{\neq}}{R}}$, for uni-molecular (viii)

Where $\Delta G^{\neq}$, $\Delta H^{\neq}$ and $\Delta S^{\neq}$ stand for Gibbs energy

change, enthalpy change and entropy change for reaction between reactant(s) and transition state.

RESULT AND DISCUSSION

Geometry

All the optimized stationary points (reactants, van der Waals complexes, intermediates, transition states and products) are presented in Tables 1 and 2. These tables show variations in bond lengths and bond angles as the reaction progresses through the intermediates and transition state to the product.

As shown in Table 1, the single C9-N10 bond length is marginally decreased while transforming from INT1 to INT2 as the partial bond is formed at van der Waal complex 2, eventually resulted in double bone at INT2 (C7-N2). Afterward, the bond shows a slight extension as the partial bond fission initiated at TS1 is fully broken at the final product P. A consecutive decrease and increase is observed as C9-C12 tries to accommodate the alterations occasioned by INT2 and TS1 formations. While C12-N1 and C12-O1 bonds are getting relatively stable throughout the transformation, C13-N10 and C8-N10 bonds are found to have consecutive decrease and increase in their lengths. Furthermore, C13-N3 and C7-C23 partial bonds initiated at the first transition state TS1 are fully established at the final product with appreciable bond length decrease, while the bond length character for multiple is lost as the C23-N3 double bond is partially cleaved to single bond in the final product. As there is no leaving group throughout the transformation, no appreciable bond angle contraction is observed. Nevertheless, there is a significant bond angle increase due to consolidation on the new bond formed as the process progresses from first transition state to the final product (Table 2 above).

Thermodynamics and Kinetics

Reaction enthalpy, entropy, Gibbs energy (for consecutive steps), and activation enthalpy, entropy of activation including Gibbs energy of activation (for transition steps) of the formation of 1'-((((aminooxy) carbonyl)amino)methyl)-2'-(1-hydroxynaphthalen-2-yl)-2'-methyl-1',2',5',6',7',7a'-hexahydrospiro[indoline-3,3'-pyrrolo[1,2-a]imidazole-2-one were evaluated, and the results are presented in Table 3. Collision frequency, activation energy, rate constant and equilibrium constant values of the isatin-L-pyrole-(Z)-2-(1-(2-hydroxy-naphthalen-1-yl)ethylidene)hydroxycarboxamide reaction system are presented in Table 4. In these tables A represents indoline-2,3-dione, B is pyrrolidine-2-carboxylic acid, while C represents (Z)-2-(1-(2-hydroxynaphthalen-1-yl) ethylidene)hydroxycarboxamide. Also VCW1 is first van der Waal complex, INT1 is 1-(3-hydroxy-2-oxoindolin-3-yl)pyrrolidine-2-carboxylic acid, VWC2 is second van der Waal complex 2, INT2 is 1-(2-oxoindolin-3-ylidene) pyrrolidin-1-ium, TS1 is first transition state and P1 and P2 are minor and major products, respectively.

As presented in Table 3, the computation for the first reversible step between the reactants and the first van der Waals complex was hugely exothermic but slightly endergonic. The entropy change for activation and the standard entropy change indicated a good interaction between reacting species in the steps leading to the formation of all the stationary points including the only transition step. This observation is also supported by the pre-exponential factors for these steps. Similar thermodynamic requirement was observed for the consecutive steps linking the reactants with the first intermediate specie, but it has almost the same exothermicity and endergonicity. In addition, the next reversible step leading to the formation of the second van der Waals complex was thermodynamically favored as it has low entropy, enthalpy and Gibbs energy values. Though exergonic, the resulting consecutive step was endothermic with increased entropy change. Furthermore, the only transition step in the three-step reaction scheme was found to be endothermic and endergonic, however with a decreased entropy change. Expectedly, the first and the only transition step in the three-step mechanism was found to be the rate determining step (Table 4). The equilibrium constant value for the bimolecular transition step collaborate this suggestion.

Furthermore, the potential energy profile (Fig. 3) suggests that the overall reaction is exothermic with low energy barrier, suggesting that it is thermodynamically feasible.

Profile of spirro heterocycle using indoline-2,3-dione, pyrrolidine-2-carboxylic acid and (Z)-2-(1-(2-hydroxy-naphthalen-1-yl)ethylidene)hydroxycarboxamide reaction

Table 1. Variations in Bond Lengths (Å) During Transformation Through INT1, INT2, TS1 and P for Indoline-2,3-dione, pyrrolidine-2-carboxylic Acid and (Z)-2-(1-(2-Hydroxynaphthalen-1-yl)ethylidene) hydroxycarboxamide Reaction System

INT1	Bond length	INT2	Bond length	TS1	Bond length	P	Bond length
C9,N10	1.456	C7,N2	1.368	C7,N2	1.413	C22,N8	1.465
C9,C12	1.576	C7,C8	1.468	C7,C8	1.392	C22,C21	1.571
C12,N1	1.380	C8,N1	1.399	C8,N1	1.378	C21,N4	1.385
C13,N10	1.475	C13,N2	1.321	C13,N2	1.343	C26,N8	1.415
C8,N10	1.454	C10,N2	1.505	C10,N2	1.481	C23,N8	1.473
C12,O1	1.212	C8,O1	1.236	C8,O1	1.327	C21,O3	1.215
				C13,N3	1.973	C26,N1	1.404
				C7,C23	3.626	C22,C11	1.592
				C23,N3	1.319	C11,N1	1. 484

Table 2. Variations in Bond Angles During Transformation Through INT1, INT2, TS1, and P for Indoline-2,3-dione, Pyrrolidine-2-carboxylic Acid and (Z)-2-(1-(2-Hydroxynaphthalen-1-yl)ethylidene)hydroxyl-carboxamide Reaction System

INT1		INT2		TS1			P
∠C12C9N10	108.19˚	∠C8C7N2	122.95˚	∠C8C7N2	126.30˚		
∠C12C9C3	101.81˚	∠C8C7C2	109.01˚	∠C8C7C2	107.35˚		
∠C3C9N10	117.46˚	∠C2C7N2	128.00˚	∠C2C7N2	126.13˚		
∠C13N10C8	111.47˚	∠C13N2C10	110.11˚	∠C13N2C10	113.42˚	∠C13N10C8	109.59˚
∠C9N10C13	117.95˚	∠C7N2C13	129.25˚	∠C7N2C13	125.05˚		
∠C8N10C9	119.00˚	∠C10N2C7	120.54˚	∠C10N2C7	121.47˚	∠C10N2C7	121.76˚
				∠C23C7N2	67.50˚	∠C23C7N2	103.03˚
				∠N2C23C7	73.61˚	∠N2C23C7	101.09˚

system was obtained by plotting electronic energy (potential energy) calculated at DFT level for all the stationary points against the reaction coordinates. The profile is presented in Fig. 2, where (A+B), VWC1, INT1, VWC2, (INT2+P1), TS1 and P on the saddle points are the reactants, van der Waals complex 1, intermediate 1, van der Waals complex 2, intermediate 2 including minor product, transition state 1 and the major product respectively.

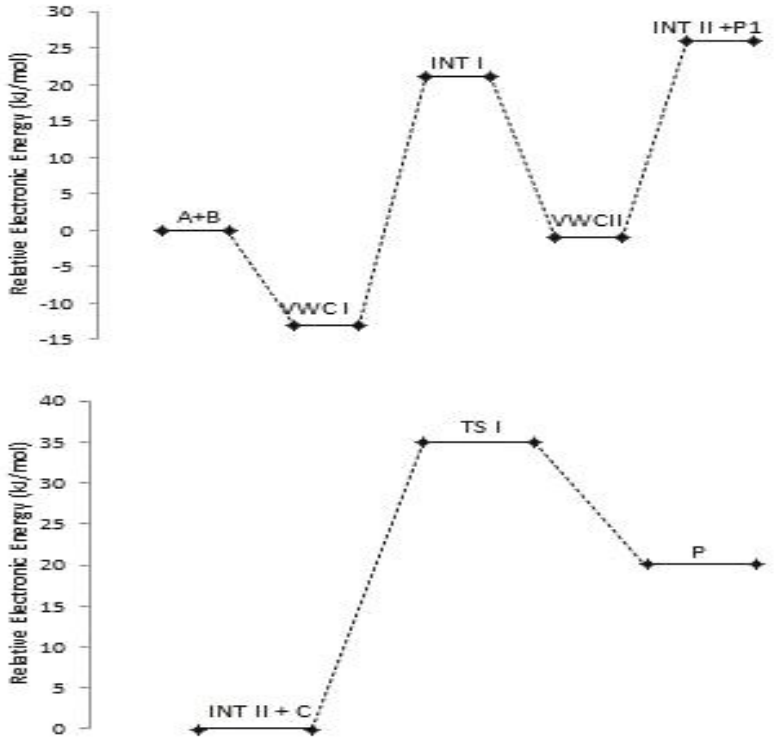

Fig. 2. Diagram of relative electronic energies along the reaction channel between indoline-2,3-dione, pyrrolidine-2-carboxylic acid and (Z)-2-(1-(2-hydroxynaphthalen-1-yl)ethylidene)hydroxyl-carboxamide reaction system**.**

The Laws of Mechanisms and Eeaction Rates

From the general reaction scheme above, the reaction mechanism consists of the following elementary steps:

$$A + B \underset{k'_{-2}}{\overset{k'_2}{\rightleftharpoons}} AB^{\#}$$

$$AB^{\#} \xrightarrow{k_2} C$$

$$C \underset{k'_{-1}}{\overset{k'_1}{\rightleftharpoons}} C^{\#}$$

$$C^{\#} \xrightarrow{k_1} D$$

$$D + E \underset{k'_{-2'}}{\overset{k'_{2'}}{\rightleftharpoons}} DE^{\#}$$

$$DE^{\#} \xrightarrow{k_{2'}} P$$

$$\frac{d[P]}{dt} = k_{2'}[DE^{\#}] \quad (1)$$

$$\frac{d[DE^{\#}]}{dt} = -k''_2[DE^{\#}] - k''_{-2}[DE^{\#}] + k''_2[D][E] \quad (2)$$

$$\frac{d[D]}{dt} = k'_1[C^{\#}] + k''_{-2}[DE^{\#}] - k''_2[D][E] \quad (3)$$

$$\frac{d[C^{\#}]}{dt} = -k_1[C^{\#}] - k'_{-1}[C^{\#}] + k'_1[C] \quad (4)$$

$$\frac{d[C]}{dt} = k'_{-1}[C^{\#}] + k_2[AB^{\#}] - k'_1[C] \quad (5)$$

$$\frac{d[AB^{\#}]}{dt} = k'_2[A][B] - k'_{-2}[AB^{\#}] - k_2[AB^{\#}] \quad (6)$$

Table 3. Thermodynamics Parameters Calculated at the B3LYP (6-311+G**) Level for the Formation of Spiroheterocycle from Indoline-2,3-dione, Pyrrolidine-2-carboxylic Acid and (Z)-2-(1-(2-Hydroxynaphthalen-1-yl) ethylidene)hydroxycarboxamide at 298.15 K

Steps	$\Delta S^{\neq}_{reaction}$ (J mol^{-1} K^{-1})	$\Delta H^{\neq}_{reaction}$ (kJ mol^{-1})	$\Delta G^{\neq}_{reaction}$ (kJ mol^{-1})	$\Delta S^{\circ}_{reaction}$ (J mol^{-1} K^{-1})	$\Delta H^{\circ}_{reaction}$ (kJ mol^{-1})	$\Delta G^{\circ}_{reaction}$ (kJ mol^{-1})
A + B ⇔ VWC1	-250.63	-72.95	+1.78			
A+B→INT1				-247.15	-36.07	+37.62
INT1 ⇔ VWC2	-0.34	-27.22	-27.12			
INT1→INT2+P1				+210.43	+48.29	-14.45
INT2 + C ⇔ TS1	-256.61	+69.71	+76.58			
INT2 + C→P2				-271.02	+241.91*	-322.71*

Table 4. Kinetic Parameters Calculated at the B3LYP (6-311+G**) Level for the Formation of Spiroheterocycle from Indoline-2,3-dione, Pyrrolidine-2-carboxylic Acid and (Z)-2-(1-(2-Hydroxynaphthalen-1-yl) ethylidene)hydroxycarboxamide at 298.15 K

Steps	A	k_2 (dm^3 mol^{-1} s^{-1})	K_2	k_1 (s^{-1})	K_1
A + B ⇔ VWC1	3.72 dm^3 mol^{-1} s^{-1}		4.89×10^{-1}		
A+B→INT1		3.04×10^{12}			
INT1 ⇔ VWC2	1.62×10^{13} s^{-1}				5.64×10^{4}
INT1→INT2+P1				3.50×10^{17}	
INT2+C ⇔ TS1	1.81 dm^3 mol^{-1} s^{-1}		3.84×10^{-14}		2.78
INT2+C→P2		2.39×10^{-1}			

Using steady state approximation Eq. (2) can be written as:

$$-k_{2'}[DE^{\#}] - k''_{-2}[DE^{\#}] + k''_2[D][E] = 0$$

$$[DE^{\#}] = \frac{k''_2}{k_{2'}+k''_{-2}}[D][E] \quad (7)$$

From Eq. (3), $k'_1[C^{\#}] + k''_{-2}[DE^{\#}] - k''_2[D][E] = 0$

$$k'_1[C^{\#}] + k''_{-2}\left(\frac{k''_2}{k_{2'}+k''_{-2}}\right)[D][E] - k''_2[D][E] = 0$$

$$k'_1[C^{\#}] = -k''_{-2}\left(\frac{k''_2}{k_{2'}+k''_{-2}}\right)[D][E] + k''_2[D][E]$$

$$[C^{\#}] = \frac{k''_2 k_{2'}}{k'_1(k_{2'}+k''_{-2})}[D][E] \quad (8)$$

From Eq. (4),

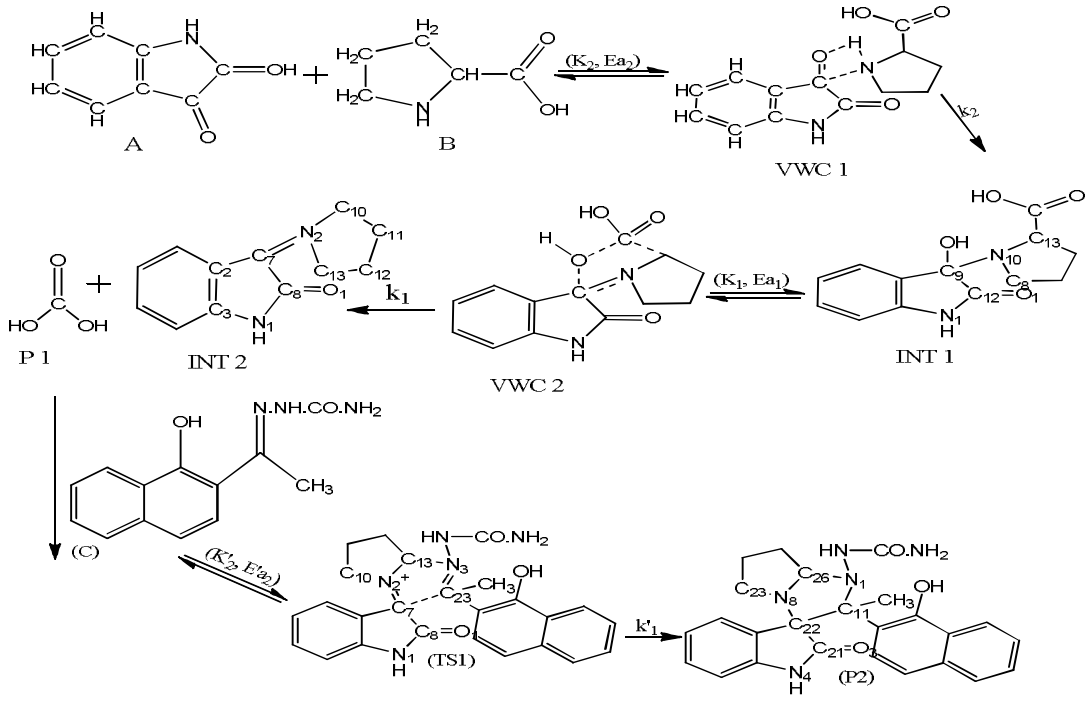

Fig. 3. Proposed mechanism for indoline-2,3-dione, pyrrolidine-2-carboxylic acid and (Z)-2-(1-(2-hydroxy-naphthalen-1-yl)ethylidene)hydroxycarboxamide reaction system.

$$, -k_1[C^{\#}] - k'_{-1}[C^{\#}] + k'_1[C] = 0$$

$$[C] = \frac{k_1 + k'_{-1}}{k'_1}[C^{\#}] \quad (9)$$

$$[C] = \frac{k_1 + k'_{-1}}{k'_1}[C^{\#}] \quad (10)$$

From Eq. (5),

$$[C] = \frac{k''_2 k_{2'}(k_1 + k'_{-1})}{k'^2_1(k_{2'} + k''_{-2})}[D][E]$$

$$\frac{k'_{-1}k''_2 k_{2'}}{k'_1(k_{2'} + k''_{-2})}[D][E] = -k_2[AB^{\#}] + \frac{k'_1 k''_2 k_{2'}(k_1 + k'_{-1})}{k'^2_1(k_{2'} + k''_{-2})}[D][E]$$

$$-k_2[AB^{\#}] = \frac{k'_{-1}k''_2 k_{2'}}{k'_1(k_{2'} + k''_{-2})}[D][E] - \frac{k'_1 k''_2 k_{2'}(k_1 + k'_{-1})}{k'^2_1(k_{2'} + k''_{-2})}[D][E]$$

$$[AB^{\#}] = \frac{k''_2 k_{2'} k_1}{k_2 k'_1(k_{2'} + k''_{-2})}[D][E] \quad (11)$$

From Eq. (6),

$$k'_2[A][B] - k'_{-2}[AB^{\#}] - k_2[AB^{\#}] = 0$$

$$k'_2[A][B] = (k'_{-2} + k_2)[AB^{\#}]$$

$$[AB^{\#}] = \frac{k'_2}{(k'_{-2} + k_2)}[A][B] \quad (12)$$

$$\frac{k''_2 k_{2'} k_1}{k_2 k'_1(k_{2'} + k''_{-2})}[D][E] = \frac{k'_2}{(k'_{-2} + k_2)}[A][B]$$

$$[D][E] = \frac{k'_2 k_2 k'_1(k_{2'} + k''_{-2})}{k''_2 k_{2'} k_1(k'_{-2} + k_2)}[A][B] \quad (13)$$

With Eq. (13) Eq. (7) can be written as:

$$\frac{k_{2'} + k''_{-2}}{k''_2}[DE^{\#}] = \frac{k'_2 k_2 k'_1(k_{2'} + k''_{-2})}{k''_2 k_{2'} k_1(k'_{-2} + k_2)}[A][B]$$

$$[DE^{\#}] = \frac{k'_2 k_2 k'_1}{k_{2'} k_1(k'_{-2} + k_2)}[A][B] \quad (14)$$

Using Eq. (14), Eq. (1)
Becomes

$$\frac{d[P]}{dt} = \frac{k_2^2 k_2' k_1'}{k_{2'} k_1 (k'_{-2} + k_2)} [A][B],$$

where

$$\frac{k_2^2 k_2' k_1'}{k_{2'} k_1 (k'_{-2} + k_2)} = K$$

is the experimental rate constant.

CONCLUSIONS

The interactions among indoline-2,3-dione, pyrrolidine-2-carboxylic acid and (Z)-2-(1-(2-hydroxynaphthalen-1-yl)ethylidene)hydroxycarboxamide leading to the formation of1'-((((aminooxy)carbonyl)amino)methyl)-2'-(1-hydroxy-naphthalen-2-yl)-2'-methyl-1',2',5',6',7',7a'-hexahydro-spiro[indoline-3,3'-pyrrolo[1,2-a]imidazole-2-one have been investigated computationally. The reaction proceed via five stationary points; two of which are van der Waals complexes, two intermediates and one transition state. The entropy change values indicated an appreciable interaction or overlap within the reacting molecules. This interaction was also supported by the variations in the geometries of the optimized species as the reaction progressed from the intermediates through the transition state to the final product. The limiting step for the reaction was the only transition step as shown by the rate and equilibrium constant values. Also, the reaction is spontaneous overall, though the transition state step was found to be non-spontaneous.

REFERENCES

[1] Longeon, A.; Guyot, M.; Vacelet, J., Araplysillins-I and-II: Biologically active dibromotyrosine derivatives from the sponge Psammaplysilla arabica. Experentia **1990**, *46*, 548-550.

[2] Ananiev, E. D.; Ananieva, K.; Abdulova, G.; Christova, N.; Videnova, E., Effect of abamectin on protein and RNA synthesis in primary leaves of Cucurbita pepo L. (zucchini). *Bulg. J. Plant Physiol*,; **2002**, *28*, 85-91.

[3] Yokosuka, A.; Mitsuno, J.; Yui, S.; Yamazaki, M.; Mimaki, Y., Steroidal Glycosides from Agave utahensis and Their Cytotoxic Activity. *J. Natural Product*, **2009**, *72*, 1399-1404.

[4] McMorris, T. C.; Chimmani, R.; Alisala, K.; Staake, M. D.; Banda, G.; Kelner, M. J., Structure-activity studies of urea, carbamate, and sulfonamide derivatives of acylfulvene (2010). *J. Medicinal Chem.,* **2010**, *53*, 1109-1116.

[5] Whang, J.; Song, Y. H., Synthesis of Thienotriazolopyrimidine Derivative Containing Triazolothiadiazole Moiety. *J. Heterocyclic Chem.* **2013**, *50*, 603-607.

[6] Nilo, Z.; Simone, S. A.; Josiane, M. S.; Liana, S. F.; Helio, G. B.; Marcos A. P. M., Regioselective synthesis and characterization of new 3-aryl-7-trifluoromethyl-[1,2,4]triazolo[4,3–**a**]pyrimidines. *J. Heterocyclic Chem.* **2011**, *48*, 1085-1090.

[7] Laragh, J. H.; Sealey, J. E., K+ Depletion and the Progression of Hypertensive Disease or Heart Failure: The Pathogenic Role of Diuretic-Induced Aldosterone Secretion Hypertension, **2001**, *37*, 806-810. DOI: 10.1161/01.HYP.37.2.806.

[8] Scholastica M. V.; Indumathi, U.; Augustine A. P. T., Synthesis, characterization and biological activity of novel spiroheterocycles from semicarbazones, Der Pharma Chemica, (2012), 4(5):1906-1912.

[9] Hehre, Warren J., A Guide to Molecular Mechanics and Quantum Chemical Calculations. Irvine, California: Wavefunction, Inc. (2003) pp. 40-47.ISBN 1-890661-18-X.

[10] Curtis, L. A.; Redfern, P. C.; Raghavachari, K.; Rassolov, V.; Pople, J. A., Gaussian-3 theory using reduced Møller-Plesset order Journal of chemical Physics, **1990**, *110*, 4703- 09.

[11] Gonzalez, C.; Schlegel, H. B., An improved algorithm for reaction path following Journal of Physical Chemistry, **1969**, *90*, 2154.

[12] Engel, T. and Reid, P. (2006). Physical Chemistry, Pearson Prentice Hall, Upper Saddle River, NJ. P. 924.